Prepared for submission to JCAP

Resolving primordial physics through correlated signatures

Kari Enqvist[1], **David J. Mulryne**[2], **Sami Nurmi**[1]

[1] University of Helsinki and Helsinki Institute of Physics, P.O. Box 64, FI-00014, Helsinki, Finland

[2] School of Physics and Astronomy, Queen Mary University of London, Mile End Road, London, E1 4NS, UK

E-mail: kari.enqvist@helsinki.fi, d.mulryne@qmul.ac.uk, sami.nurmi@helsinki.fi

Abstract. We discuss correlations among spectral observables as a new tool for differentiating between models for the primordial perturbation. We show that if generated in the isocurvature sector, a running of the scalar spectral index is correlated with the statistical properties of non-Gaussianities. In particular, we find a large running will inevitably be accompanied by a large running of $f_{\rm NL}$ and enhanced $g_{\rm NL}$, with $g_{\rm NL} \gg f_{\rm NL}^2$. If the tensor to scalar ratio is large, a large negative running must turn positive on smaller scales. Interestingly, the characteristic scale of the transition could potentially distinguish between the inflaton and isocurvature fields.

1 Introduction

Recently an unprecedented amount of data has become available to constrain the properties of primordial fluctuations which source structure in our universe. This includes the results from the Planck satellite [1, 2, 3], the BICEP2 collaboration [4], and the South Pole Telescope (SPT)[5], as well as many others. Single field slow roll inflation, based on a scalar field, the inflaton, appears compatible with all the data. However, in addition to the inflaton, there might be other scalars present during inflation. Indeed, unless the Standard Model couplings are drastically modified at inflationary energies, we know that there is at least one light isocurvature scalar, the Higgs, which was present during inflation and acted as a spectator field [6, 7, 8, 9, 10, 11].

While the SM Higgs appears to have little impact on primordial perturbations, see however [12, 13], isocurvature fields in general could play a significant role if an efficient curvaton-type conversion into adiabatic perturbations takes place. Here we take curvaton-type to cover in addition to the curvaton scenario [14, 15, 16, 17, 18] also all other models where isocurvature fields can be converted efficiently into adiabatic perturbations, e.g. modulated reheating [19, 20] and modulated end of inflation [21]. The Planck bound on non-Gaussianity $f_{\rm NL}^{\rm local} = 2.7 \pm 5.8$ (68% CL) alone places stringent constraints on curvaton-type fields as the dominant source of primordial perturbations, see e.g. [22, 23, 24, 25, 26]. Moreover, as is well known, this would be ruled out entirely by an eventual detection of large amplitude primordial gravitational waves. Constraints, however, are significantly weaker for an admixture of curvaton and inflaton sourced perturbations [27, 28, 29, 30]. The question then arises: given the data, how one could most efficiently constrain, or possibly detect, additional scalars such as the curvaton?

Here we pursue one possible avenue and point out that correlations between the observed signatures of the primordial perturbation could provide a new handle on the dynamics during inflation. Given that leading order effects in slow-roll are well understood, our focus is what new can be learnt from effects at second order, and what a detectable running of the scalar spectral index, denoted by α, could tell us. In particular, we will investigate the information encoded in the mutual dependence of non-Gaussian statistics and the lowest order running of the scalar spectral index. As we will demonstrate, a large α would signal the presence of features in the potential, which in turn would give rise to a different structure of non-Gaussianities for the pure inflaton and the mixed inflaton-curvaton models, thus making it possible to distinguish between the two.

In general, there are two options for the origin of large running, $|\alpha| = \mathcal{O}(n_s - 1)$, of the spectral index. The first lays the responsibility with the inflaton potential. All that is required in this case is that the inflaton's third slow-roll parameter, ξ, becomes of $\mathcal{O}(n_s - 1)$. The conventional assumption is that $|\xi| = \mathcal{O}((n_s - 1)^2)$. As emphasised by Stewart [31], however, this is a superfluous assumption often made in slow-roll inflation for reasons of convenience only. It greatly simplifies calculations, and is satisfied by the simplest inflationary potentials, but it is not required by general inflationary dynamics.

The second possibility for generating a large running is that the potential of a curvaton type isocurvature field gives rise to the running. This option has recently been studied by Takahashi [32] using a curvaton scenario as a concrete example. The idea was then revisited in light of the BICEP2 data by Sloth [33].

As we will see, the latter case leads to distinct signatures in the non-Gaussian statistics, while in the former non-Gaussianity remains negligible. Moreover, we find that there is a

further difference between the two cases for examples in which the running is accompanied by a significant gravitational wave signal. If the large running is accompanied by a significant tensor to scalar ratio r, this *implies that the potential contains a feature*. This feature is not required to violate slow-roll, but the condition required on the third slow-roll parameter cannot be maintained for many e-folds, implying that a negative running on the pivot scale has to be accompanied by a positive running on shorter scales. This would correspond to a feature of a specific type in the potential, but with differing constraints on the feature in the inflaton and isocurvature cases.

Observational bounds on the running parameter α are relatively weak. Interestingly, however, there have been several reports of hints for a sizeable running. Analysis of the SPT data implies a preference for $\alpha = -\mathcal{O}(n_s - 1)$ at the 2σ level [5]. More recently the BICEP2 collaboration [4] detected a significant B-mode signal in CMB data, which however now looks to be mostly or even entirely due to galactic dust [34]. However, if the joint analysis of Planck and BICEP2 data currently in progress (or any future instrument such as BICEP3, Keck, Spider or PIPER [35, 36, 37, 38]), did reveal a primordial component in the signal, the discovery would likely favour a sizeable running of the spectral index, see for example Refs. [4, 39]. In the more distant future, surveys of spectral distortions could significantly extend the currently accessible window of $\Delta N \sim 7$ inflationary e-folds. Progress of 21-cm cosmology could extend the window even further. This would open up entirely new possibilities to efficiently probe the scale dependence of the spectrum.

It is therefore of great interest to carefully address second order effects such as the running of spectral indices, and to address the question: *if a scenario generates a significant running, are there further observational consequences that would result?* This is the primary aim of the present study.

The structure of the paper is as follows. In § 2 we discuss large running generated by a feature in the inflaton potential. This is contrasted to the isocurvature case in § 3, where we analyse large running from an isocurvature field and its correlation with non-Gaussianities. In § 4 we present and analyse numerically two illustrative examples of curvaton models where features in potential generate a large running. We conclude in § 5.

2 Running from the inflaton field

Let us consider first the running generated by single field inflation. In this case, for a given inflaton potential, $V(\phi)$, the tensor to scalar ratio, r, the spectral index, n_s, and the running, α, are given by the expressions

$$\begin{aligned} r &= = 16\epsilon\,, \\ n_s - 1 &= -6\epsilon + 2\eta + 1.062\xi + \dots\,, \\ \alpha &= 16\epsilon\eta - 24\epsilon^2 - 2\xi + \dots\,, \end{aligned} \tag{2.1}$$

where the slow-roll parameters are

$$\begin{aligned} \epsilon &= M_{\rm P}^2 \frac{V'^2}{2V^2}\,, \\ \eta &= M_{\rm P}^2 \frac{V''}{V}\,, \\ \xi &= M_{\rm P}^4 \frac{V'V'''}{V^2}\,. \end{aligned} \tag{2.2}$$

The additional terms in Eq. (2.1) are here taken to be negligible on the assumption that slow-roll parameters beyond ξ are subdominant compared to the first three. In models in which ξ is of order ϵ or η, however, this is not the case in general. A quantitative analysis then requires a generalised slow-roll expansion [31, 40], or a numerical analysis. The above expressions are however sufficient for a qualitative discussion. Considering Eqs. (2.1), we find that in the absence of a fine tuned cancelation, ϵ, and η need to be $(n_s - 1) \sim 0.01$ or much smaller, in order that the spectral index can take a value in the observationally preferred range $n_s = 0.96 \pm 0.007$ [3]. It is necessary, therefore, that ξ be of a similar magnitude, if the running is also to be $\mathcal{O}(n_s - 1)$.

Assuming the potential supports a positive ξ of this amplitude for at least a few e-folds, the fact that $\mathrm{d}\eta/\mathrm{d}N \sim -\xi$ implies that η will change by at least at few times $\mathcal{O}(\xi)$. After the phase of evolution which generates such a large negative running, therefore, barring fine tuned cancelations, η will be negative even if it was positive at the start of this phase. Such a negative η also feeds an increase in the rate at which ϵ increases *if ϵ is large enough for r to be significant*, through the equation $\mathrm{d}\epsilon/\mathrm{d}N = -2\epsilon(\eta - 2\epsilon)$. The implication then is that the inflation would not last sufficiently long if such a behaviour continues. This will be made more transparent below. After a few e-folds of this kind of a behaviour, a decrease in ϵ is needed for the potential to be able to generate a sufficient number of e-folds of inflation.

Such a decrease requires a positive η with $\eta > 2\epsilon$, so the mass of the potential must switch back to positive. This in turn requires a large negative ξ and a hence a large positive running. Again barring fine tuning, therefore, potentials which realise a large negative running on the pivot scale must have a large positive running on shorter scales, and must possess an inflection point. For example, the potentials considered by Takahashi and collaborators [41, 42] consisted of a series of inflection points. This behaviour implies that on shorter scales the spectral index must evolve towards bluer values. Such behaviour is potentially observable though joint analysis of CMB and LSS data, or possibly on even shorter scales by virtue of CMB spectral distortions [43] if the spectral index actually becomes blue. The condition required for this to occur is mildly stronger than the condition for the growth of ϵ, since it requires $\eta > 3\epsilon$. However, in concrete models this condition may well be realised, potentially leading to a correlated signature to a negative running on the pivot scale. A spectrum which is blue tilted for an range of scales shorter is indeed what occurs in the model of Ref. [42].

2.1 Explicit parametrisation of the inflaton feature

With the preceding discussion in mind, let us therefore consider the running generated by single field inflation with an inflection point in the inflaton's potential. For convenience we parameterise the potential around an inflection point as

$$V(\phi) = V_0 \left(1 + b\left(\frac{\phi - \phi_0}{\phi_0}\right) + c\left(\frac{\phi - \phi_0}{\phi_0}\right)^3 + \dots\right) , \tag{2.3}$$

and we assume $b > 0$ and $c > 0$. At the inflection point the slow roll parameters are given by

$$\epsilon_0 = \frac{b^2}{2}\left(\frac{\phi_0}{M_{\rm P}}\right)^{-2} , \tag{2.4}$$

$$\eta_0 = 0 , \tag{2.5}$$

$$\xi_0 = 6cb\left(\frac{\phi_0}{M_{\rm P}}\right)^{-4} . \tag{2.6}$$

Here we concentrate on the case $\xi_0 \gg \epsilon_0^2$ where a large negative running $\alpha_0 \simeq -2\xi$ is generated at the inflection point. Assuming the higher order terms in (2.3) are negligible, the slow roll inflation can be sustained only for a limited range of e-folds

$$N_{\rm max} = \frac{1}{\sqrt{|\alpha_0|}}\left(2\arctan(x_{\rm e}) - \frac{r_0}{12\sqrt{|\alpha_0|}}\left(x_{\rm e}^2 + 2\ln(1+x_{\rm e}^2)\right)\right) \ , \qquad x_{\rm e} = \sqrt{\frac{3c}{b}}\,\frac{\phi_0 - \phi_{\rm e}}{\phi_0} \tag{2.7}$$

In the limit of large gravitational waves $r_0 > 4|\alpha_0|$ the slow roll ends as $\epsilon(\phi_e) = 1$ and the corresponding field value is determined by the condition

$$x_{\rm e}^2 + \sqrt{\frac{r_0}{|\alpha_0|}}\left(x_{\rm e} + \frac{1}{3}x_{\rm e}^3\right) = \frac{4}{\sqrt{r_0}} - 1 \ . \tag{2.8}$$

For $r_0 = 0.2$ and $\alpha_0 = 0.02$ this yields $N_{\rm max} \lesssim 10$. Decreasing the running and the tensor-to-scalar ratio to $r_0 = 0.1$ and $\alpha_0 = 0.01$ increases the number of e-folds up to $N_{\rm max} \lesssim 15$.

Therefore, if $r = \mathcal{O}(0.1)$ and $\alpha = \mathcal{O}(n_s - 1)$ at the horizon crossing of observable modes the potential (2.3) necessarily needs to be flattened out by higher order terms within $N = \mathcal{O}(10)$ e-folds. The flattening essentially requires a second inflection point and a subsequent evolution of η to positive values. This will push the spectral index n_s towards, and possibly over, to blue tilted values, as discussed above.

It would be interesting to investigate how generically blue values will be reached, and if this effect, which necessarily follows from the large running and large tensor-to-scalar ratio in single field models of the form (2.3), could be detectable through future observations of LSS, CMB spectral distortions or 21-cm cosmology. However, we defer a detailed study to future work. Examples of this behaviour in models with a large running can be found in for example Refs. [40, 42]

3 Running from an isocurvature field

Let us now consider the case where more than one light field is present during inflation. In this case the running can be generated by isocurvature fields which after the end of inflation convert their fluctuations into adiabatic perturbations.

Using the δN formalism [44, 45, 46, 47, 48] the spectral index to lowest order in slow roll is given by

$$n_s - 1 = -2\epsilon^* - 2\frac{1 - \eta_{ab}N_aN_b}{N_cN_c} + \dots \ . \tag{3.1}$$

Here N_a are the derivatives of N defined in the usual way [48], and the subscript Roman letters run over all light fields present. In a similar manner to the single field case, however, additional terms in Eq. (3.1) cannot in general be neglected if the running is significant. Here we will use expressions such Eq. (3.1) only to guide us in analytical estimates, but where necessary use numerical analysis which does not rely on them.

Differentiating this expression with respect to $\ln k = \ln(aH)$ provides an expression for the running, and one finds

$$\frac{{\rm d}n_s}{{\rm d}\ln k} \supseteq -\frac{2}{N_fN_f}\frac{\xi^*_{ac}N_aN_c}{N_fN_f} + \dots \tag{3.2}$$

where $\xi_{ab} = V_{abc}V_c/V^2$. As in the single field case, to enhance running while adhering to slow-roll typically requires $\xi = \mathcal{O}(\epsilon)$, while in the simplest models $\xi = \mathcal{O}(\epsilon^2)$. In this section

we consider two field models, and the consequences of a large $\xi_{\chi\chi}$, where χ is considered to be a field which is a spectator at horizon crossing. This will lead to a large running if the perturbation in this field is converted into a curvature perturbation. We now discuss the conditions needed for the enhancement of the running, as well as the number of e-folds over which such an enhancement can be maintained.

3.1 Explicit parametrisation of the isocurvature feature

In a manner similar to the inflaton case above, we consider a potential for the isocurvaure field χ expanded about an inflection point, given by

$$U(\chi) = U_0 \left(1 + \beta \left(\frac{\chi - \chi_0}{\chi_0}\right) + \gamma \left(\frac{\chi - \chi_0}{\chi_0}\right)^3 + \dots\right) \ . \tag{3.3}$$

Here U_0, β and γ are constants and we take the full scalar potential to be of the form $V = V(\phi) + U(\chi)$.

In order to be an isocurvature field, χ should be energetically subdominant and the gradient of the full potential in χ direction should vanish to first order in slow roll

$$\Omega_\chi = \frac{U}{3H^2 M_{\rm P}^2} \ll 1 \ , \qquad \epsilon_\chi \lesssim \epsilon_H^2 \ . \tag{3.4}$$

A conversion of the isocurvature fluctuations of χ into adiabatic perturbations after inflation could generate a sizeable running of the spectral index, as suggested by Takahashi [32] and Sloth [33]. In the examples considered here, the eventual magnitude of the running is controlled by the c in the potential (3.3) expanded around the inflection point. Assuming the third derivative of the inflaton potential is negligible, the running generated through the isocurvature field at scales exiting the horizon as $\chi = \chi_0$ is given by

$$\alpha_0 = -2 w_\chi \xi_{\chi\chi} + \mathcal{O}(\epsilon_H^2) \ , \qquad \xi_{\chi\chi} = 12\, b\, c\, \Omega_\chi^2 \left(\frac{M_P}{\chi_0}\right)^4 \ . \tag{3.5}$$

Here $w_\chi = \mathcal{P}_\chi / \mathcal{P}_\zeta$ is the χ contribution to the total curvature perturbation at the time when the system becomes adiabatic and ζ freezes to constant. For a large tensor perturbation with $r \sim 0.1$, the isocurvature contribution could not account for the total curvature perturbation but its typical contribution is constrained by $w_\chi \lesssim 0.5$ [27, 30].

The range of χ_0 values for which the isocurvature conditions (3.4) are satisfied and a large running $|\alpha_0| \gtrsim \epsilon_{\rm H}$ can be obtained at least locally is given by

$$b \left(\frac{\Omega_\chi}{10^{-7}}\right) \left(\frac{0.1}{r}\right)^{3/2} \lesssim \frac{\chi_0}{H} \lesssim \left(\frac{\Omega_\chi}{10^{-5}}\right)^{1/2} w_\chi^{1/4} b^{1/4} \left(\frac{c}{10^{-5}}\right)^{1/4} \left(\frac{0.1}{r}\right)^{3/4} \ . \tag{3.6}$$

Moving away from the inflection point ϵ_χ will rapidly grow due to the large running. Unless the growth is leveled out by higher order terms in (3.3) the isocurvature condition (3.4) eventually gets violated as

$$\epsilon_\chi = \epsilon_{\chi_0} \left(1 + \tan^2\left(\frac{\xi_{\chi\chi}}{6} N\right)\right)^2 \simeq \epsilon_H^2 \ . \tag{3.7}$$

The corresponding maximum amount of e-folds after the inflection point under which χ remains an isocurvature field is given by

$$N_{\rm max} \simeq \sqrt{\frac{4w_\chi}{|\alpha_0|}} \arctan\left(\sqrt{\frac{\epsilon_H^2}{\epsilon_{\chi 0}} - 1}\right) < \pi\sqrt{\frac{w_\chi}{|\alpha_0|}} \tag{3.8}$$

Taking $\alpha_0 \sim 0.01$ with $w_\chi \lesssim 0.5$ as a representative example we find

$$N_{\rm max} \lesssim 30 \ , \tag{3.9}$$

no matter how small the isocurvature slope $\epsilon_{\chi 0}$ would be at the inflection point. In order to keep χ as an isocurvature field, its potential necessarily needs to be levelled out by higher order terms in (3.3) within the $N \sim 30$ e-folds after the inflection point.

We therefore find that a single feature in the isocurvature potential is in general not enough to generate a large running $|\alpha| \sim 0.01$ while still keeping the isocurvature field decoupled from the adiabatic direction over the observable $N_{\rm CMB} \sim 60$ e-folds. It appears that a large running from an isocurvature field can be consistently generated only if there are multiple features in the isocurvature potential, as was the case for the inflaton potential. In both setups a large negative running $\alpha = -\mathcal{O}(n_s - 1)$ needs to be followed by a transition to positive running on smaller scales.

The characteristic scale of the transition however distinguishes the inflaton induced running from the isocurvature case. In the inflaton case the transition from positive to negative running occurs within $N \sim 10$ e-folds after the inflection point whereas for the isocurvature case the transition can take place at much smaller scales. This difference could be observable by future measurements of spectral distortions and 21-cm spectrum which are expected to significantly extend the currently observable range $\Delta N \sim 7$ of CMB scales.

3.2 Estimates of isocurvature features in $f_{\rm NL}$ and $g_{\rm NL}$

We now consider further consequences of a large running generated in the isocurvature sector. In particular, we will consider the amplitude of the reduced bispectrum $f_{\rm NL}$, and of trispectrum parameter $g_{\rm NL}$, given respectively by

$$f_{\rm NL} = \frac{5}{6}\frac{N_a N_b N_{ab}}{(N_c N_c)^2} \tag{3.10}$$

and

$$g_{\rm NL} = \frac{25}{54}\frac{N_a N_b N_c N_{abc}}{(N_d N_d)^3} \ . \tag{3.11}$$

In a multi-field inflationary model, the derivatives of N are not unrelated to one another. Rather one finds [47]

$$\frac{N_a V_a}{V} = 1 \tag{3.12}$$

and differentiating this expression

$$\frac{N_{ab} V_a}{V} = \frac{N_a V_a V_b}{V^2} - \frac{N_a V_{ab}}{V} \tag{3.13}$$

and

$$\frac{N_{abc} V_a}{V} + \frac{N_{ab} V_{ac}}{V} + \frac{N_{ac} V_{ac}}{V} + \frac{N_a V_{abc}}{V} = \frac{V_{bc}}{V} \, . \tag{3.14}$$

In a two field model in which one field is a spectator at horizon crossing, the derivative of N for the inflation field ϕ is very nearly constant from horizon crossing for the entire subsequent evolution, and is given by $|N_\phi| \approx 1/(2\epsilon_\phi^*)^{1/2}$ (with $M_{\rm P} = 1$). On the other hand, N_χ will grow from a negligible initial value if isocurvature fluctuations are converted into ζ.

We are interested in the case where N_χ does indeed grow, and moreover, in order to make analytic progress we will often consider the point at which $N_\chi \approx N_\phi$. This condition is reasonable in our study to gain an estimate of the effects of a large running, since we know the isocurvture field must contribute significantly to ζ for the running of ζ to be significant, while if there is a significant detection of gravitational waves, it must not dominate it. If N_χ came to dominate r would become negligible since

$$r = \frac{16\epsilon^*}{1+R}\,, \tag{3.15}$$

where $R = N_\chi^2/N_\phi^2$. Moreover, the condition $R = 1$ typically coincides approximately with the peak value of $f_{\rm NL}$ generated during the evolution of ζ in a two-field model [49, 50]. We see numerically that our conclusions regarding non-Gaussianity hold more generally than for the case $N_\chi \approx N_\phi$, and thus do not require a significant value of r.

Considering Eq. (3.13), and assuming $V_{\phi\chi} = 0$, we find

$$N_{\phi\chi}V_\phi + N_{\chi\chi}V_\chi = V_\chi - N_\chi V_{\chi\chi} \tag{3.16}$$

assuming there is no cancelation between the two terms on the lhs, when $f_{\rm NL}$ is large, its value when $N_\phi = N_\chi$, which is close to it peak value can be estimated by

$$\frac{6}{5}f_{\rm NL} \approx \frac{1}{2}N_{\chi\chi}\epsilon_\phi^* = \mathcal{O}\left(-\frac{\eta_{\chi\chi}}{4}\left(\frac{\epsilon_\phi^*}{\epsilon_\chi^*}\right)^{1/2}\right)\,. \tag{3.17}$$

Playing the same game with Eq. (3.14), and again assuming there is no cancellation one finds that when ξ is first order in slow-roll, as required to source a large running, then the leading term gives

$$\frac{54}{25}g_{\rm NL} \approx \frac{1}{2^{3/2}}N_{\chi\chi\chi}\epsilon^{*3/2} = \mathcal{O}\left(\frac{-\xi_{\chi\chi}^*}{8}\frac{\epsilon_\phi^*}{\epsilon_\chi^*}\right) \tag{3.18}$$

and hence

$$g_{\rm NL} = \mathcal{O}\left(-f_{\rm NL}^2\frac{\xi_{\chi\chi}}{\eta_{\chi\chi}^2}\right)\,. \tag{3.19}$$

The last expression is clearly only valid if $\eta_{\chi\chi}$ is non-zero. Consequently we see that when a large running is present we expect an enhanced value of $g_{\rm NL}$. A further consequence is a large running [51, 52, 53, 54, 55] of $f_{\rm NL}$. This is because in the same approximation

$$\frac{{\rm d}f_{\rm NL}}{{\rm d}\ln k} \supseteq -\frac{5}{6}g_{\rm NL}\frac{\sqrt{\epsilon_\chi}}{\sqrt{\epsilon_\phi}}\,. \tag{3.20}$$

As we will see this enhanced running will prove to be a constraint on otherwise viable models.

A word of caution about these expressions is in order. There are two terms on the LHS of the expressions above we use to generate our estimates for $f_{\rm NL}$ and $g_{\rm NL}$, and either or both of these can contribute towards any large value on the RHS. This means that the expressions we write down are only order of magnitude considerations, and cancellations

between terms can render them inaccurate, even altering the sign of $f_{\rm NL}$ and $g_{\rm NL}$. Applying the $f_{\rm NL}$ expression above to the simplest curvaton model with a quadratic curvaton potential, for example, gives an estimate for $f_{\rm NL}$ of the correct magnitude, but gives the incorrect sign.

Below we will see that these estimates work very well for two separate models which generate a large running (for both sign and magnitude). Never-the-less they should be regarded as useful guides rather than concrete expressions, and we will use numerical δN simulations to confirm our expectations in each case.

4 Concrete isocurvature examples

To provide concrete examples of models of inflation in which a large running is generated in the isocurvature sector together with a correlated signal in the bispectrum and trispectrum, we consider the curvaton model [14, 15, 16, 17, 18, 23, 24, 29, 56, 57, 58]. This is a two field model in which one field, which is a spectator at horizon crossing decays to radiation long after the other field which dominates the energy density during inflation. During the oscillations of this field its relative contribution to the energy density can gradually increase, and so too does the contribution of its perturbations to the curvature perturbation ζ. We restrict our attention to this model, although similar results would be expected in other two-field models, for example those which generate a large $g_{\rm NL}$ during inflation when $\xi_{\chi\chi}$ is large [59].

4.1 Oscillatory isocurvature potential

As a first a concrete example, therefore, we follow Takahashi and Sloth by considering a curvaton model where the curvaton potential has subdominant oscillations. The potential we use is given by

$$\begin{aligned} V(\phi) &= \frac{1}{2}m_\phi^2\phi^2\,, \\ V(\chi) &= \frac{1}{2}m_\chi^2\chi^2\left(1+A\cos(\chi/w)\right)\,, \end{aligned} \tag{4.1}$$

where ϕ is the inflation and χ the curvaton, and we have chosen a slightly different potential to Takahashi so as to ensure the mass at the minimum of the curvaton potential is given by m_χ.

We take $A<1$, and for $w<1$ find that potential contains successive inflection points when $\chi\approx w(1/2+2n)\pi$ and $\chi\approx w(3/2+2n)\pi$. The condition that the field does not get stuck in a local maxima requires $\chi^*<w/(2A)$. At the inflection points one finds

$$\xi_{\chi\chi}\approx\left(1\pm\frac{A\chi}{2w}\right)\frac{A\chi^3m_\chi^4}{2w^3V(\phi)^2}\,. \tag{4.2}$$

and that increasing A or m_ϕ, or decreasing ω increases ξ.

4.2 Numerical evolution

As a concrete example we take the parameters values: $m_\phi=5m_\chi$, $A=0.0001$ and $w=4\times10^{-5}$. Together with the field values when scales corresponding to the pivot scale exited the horizon (which we take to be 50 e-folds before the end of inflation): $\phi=14M_{\rm P}$ and $\chi=w(1/2{+}2{*}198)\pi M_{\rm P}$. In this example we are not being overly careful to ensure consistency

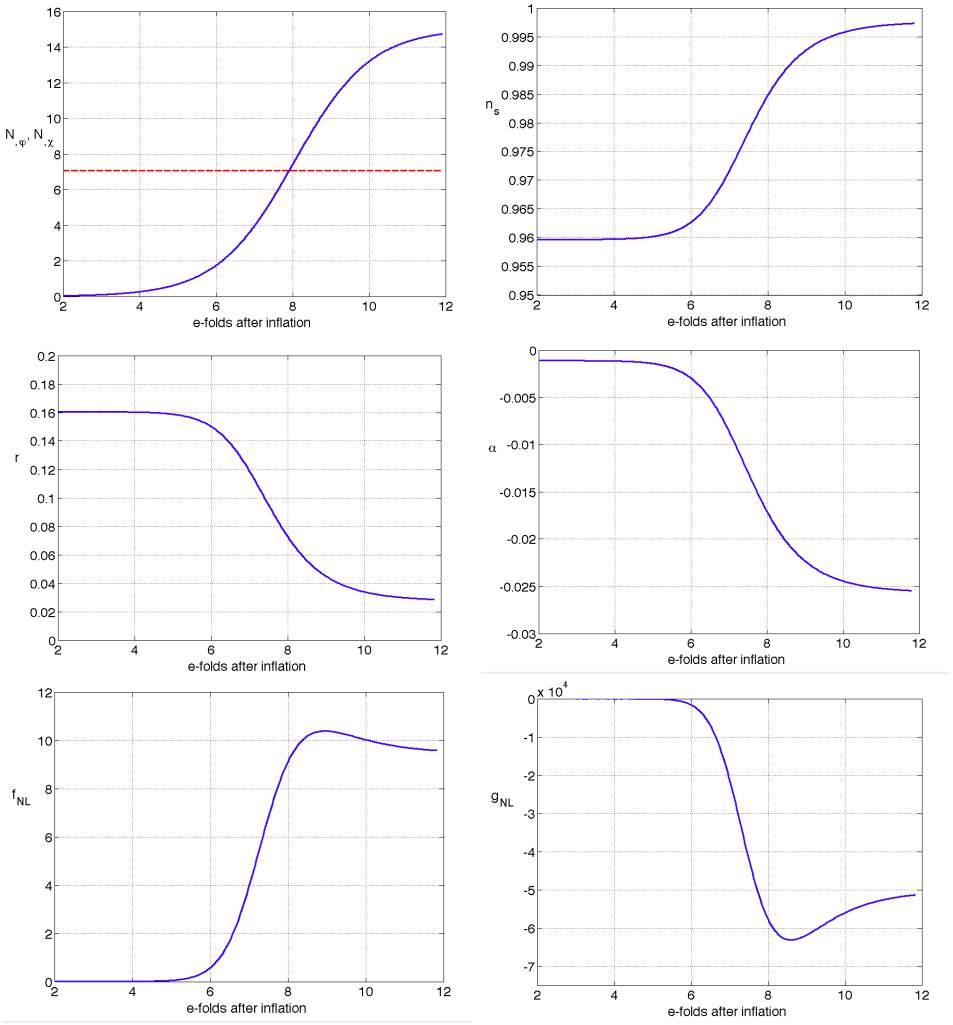

Figure 1. Results for the oscillatory isocurvature potential eq. (4.1) with $m_\phi = 5m_\chi$, $A = 0.0001$ and $w = 4 \times 10^{-5}$ and initial conditions $\phi = 14M_{\rm P}$ and $\chi = w(1/2 + 2 * 198)\pi M_{\rm P}$ set $N = 50$ e-folds before the end of inflation. The figures present the time evolution (in e-folds) from the end of inflation of N_ϕ (dashed line top left), N_χ (solid line top left), n_s (top right), r (middle left), α (middle right), $f_{\rm NL}$ (bottom left) and $g_{\rm NL}$ (bottom right).

with observation, but rather aim to illustrate the features we have been discussing for models with a significant running and significant production of gravitational waves. To generate our results we numerically evolve the covariance matrix $\langle \delta\phi_a(k)\delta\phi_b(k)\rangle$ until all scales we are interested in have exited the horizon, the method we use is described in detail elsewhere [60]. Then we relate this to the spectrum for curvature perturbation ζ by calculating the derivatives of N from the point we stop evolving the covariance matrix. To calculate non-Gaussianities, we use calculate the derivatives of N over a range of scales, from the pivot scale down to the final scale we evolve the covariance matrix for. We use the numerical method discussed in Ref. [49], with the added assumptions that the inflaton reheats instantaneously when it starts to oscillate, and that once the curvaton has undergone a large number of oscillations it may be approximated by a fluid with zero pressure.

In Fig. 1, we show how N_ϕ, N_χ calculated on the pivot scale, n_s r, α, $f_{\rm NL}$, and $g_{\rm NL}$ evolve

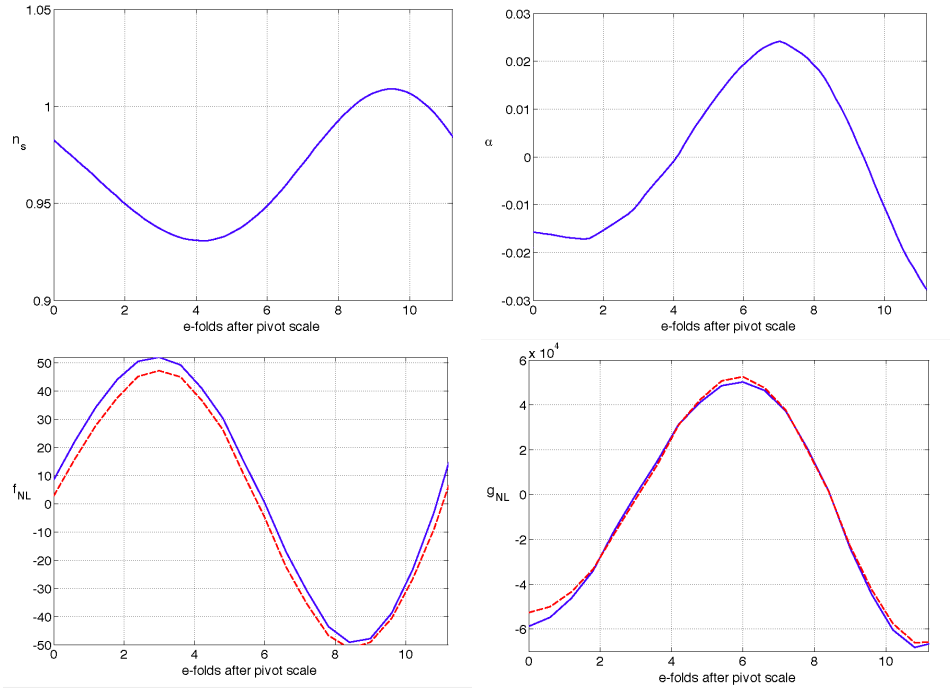

Figure 2. Results for the oscillatory isocurvature potential eq. (4.1) with $m_\phi = 5m_\chi$, $A = 0.0001$ and $w = 4 \times 10^{-5}$ and initial conditions $\phi = 14M_{\rm P}$ and $\chi = w(1/2 + 2 * 198)\pi M_{\rm P}$ set $N = 50$ e-folds before the end of inflation. The figures present the scale dependence of n_s (top left), r (top right), $f_{\rm NL}$ (bottom left solid), the estimate of $f_{\rm NL}$ (bottom right dashed), $g_{\rm NL}$ (bottom right solid) and the estimate of $g_{\rm NL}$ (bottom right dashed). The results are shown as a function of e-folds from the pivot scale $N = 50$ and measured at the point $N_\phi = N_\chi$ for the pivot scale.

during the phase of evolution in which the curvaton is oscillating about its minimum and its energy density red-shifting more slowly than that of the radiation produced by the inflaton field. In these figures different numbers of e-folds along the x axis correspond to different reheating times for the curvaton field, and hence different energy scales for the reheating. In a real model the value of the observational parameters which are realised is then fixed by the curvaton's reheating scale. Plotting the results in this way allows us to simultaneously present results for many different reheating scales at once.

In these figures one can see the almost constant N_ϕ described above, the growing N_χ, and the generation of the large running in the spectral index as the curvaton starts to contaminate the spectrum. We see in this example that at a reheating time of about 7 e-folds after inflation ends n_s is close to the observationally preferred value, and $r \approx 0.1$. As expected, α is enhanced. It is clear that there is an very enhanced value of $g_{\rm NL}$ which accompanies an enhanced α, irrespective of the value of r.

Next we plot how the observables behave as a function of horizon exit time. To do this we calculate n_s, α, $f_{\rm NL}$ and $g_{\rm NL}$ as a function of horizon exit time over the range of e-fold taken for the isocurvature field to evolve over on oscillation in the potential. We evaluate the answer at the point where the derivatives of N are equal for the pivot scale. We expect the estimates for $f_{\rm NL}$ and $g_{\rm NL}$ above to be accurate to at least at the order of magnitude level at this point. We plot the results in Fig. 2. This again clearly illustrates the correlation between $g_{\rm NL}$ and the running of the spectral index for a variety of initial conditions, in addition to

the usefulness of the estimates we have derived.

In Fig. 3, we repeat this exercise but for the case $m_\phi = 20/3 m_\chi$, $A = 0.0003$ and $w = 4 \times 10^{-5}$, and the same initial conditions. In this case the values of n_s and α are similar at horizon crossing, but the slower rate at which the isocurvature field evolves means it takes roughly twice as long in e-folds for on oscillation of the potential to be traversed. In this case the large running of $f_{\rm NL}$, and the extra e-folds over which it applies, means that $f_{\rm NL}$ becomes large over CMB scales, and this model is likely ruled out.

Finally for this case we plot the spectra of ζ directly as a function of e-folds after horizon crossing in Fig.4.

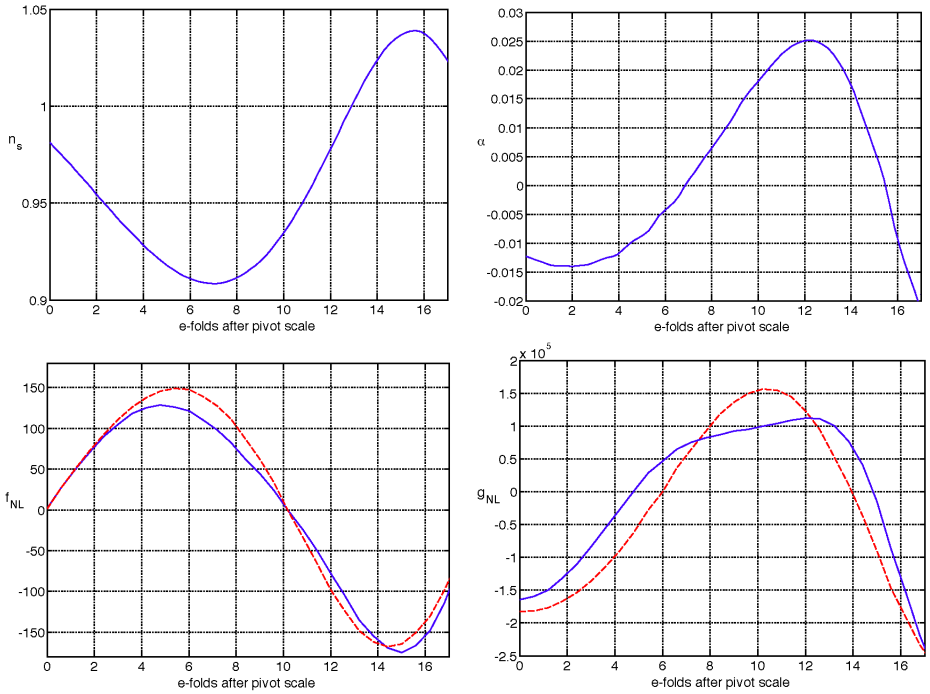

Figure 3. Results for the oscillatory isocurvature potential eq. (4.1) with $m_\phi = 20/3 m_\chi$, $A = 0.0003$ and $w = 4 \times 10^{-5}$ and initial conditions $\phi = 14 M_{\rm P}$ and $\chi = w(1/2 + 2 * 198)\pi M_{\rm P}$ set $N = 50$ e-folds before the end of inflation. The figures present the scale dependence of n_s (top left), r (top right), $f_{\rm NL}$ (bottom left solid), the estimate of $f_{\rm NL}$ (bottom right dashed), $g_{\rm NL}$ (bottom right solid) and the estimate of $g_{\rm NL}$ (bottom right dashed), as a function of e-folds from the pivot scale fixed at $N = 50$ and measured at the point $N_\phi = N_\chi$ for the pivot scale.

4.3 Piecewise isocurvature potential

As a second example, in order to have more control over the shape of the potential, we study an isolated feature rather the a continuous series as in the previous example. We therefore consider a potential of the form (3.3), including also a quartic piece in the potential, and match it to a potential of purely quadratic form about the minimum, i.e. $V = 1/2 m_\chi^2 \chi^2$. We do so by requiring that the first and second derivatives of the potential agree at some matching position χ_m. This fixes the coefficient of the quartic term, and V_0, leaving us free to adjust b and c as we wish. In particular, this allows us to arbitrary fix $\xi = M_{\rm P}^4 bc/\chi_0^4$.

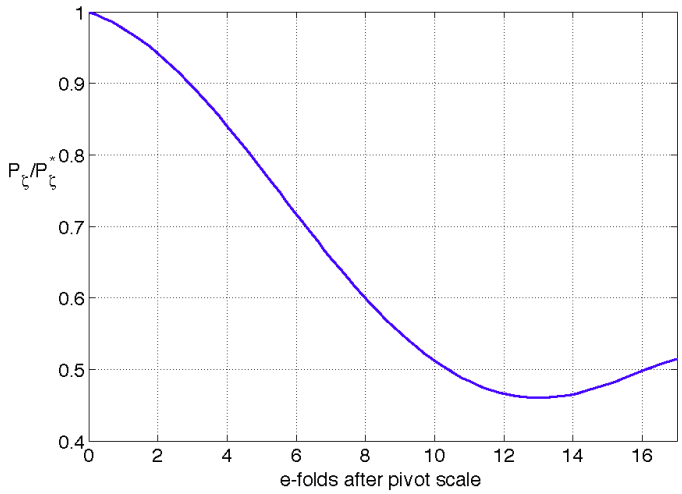

Figure 4. Results for the oscillatory isocurvature potential eq. (4.1) with $m_\phi = 20/3 m_\chi$, $A = 0.0003$ and $w = 4 \times 10^{-5}$ and initial conditions $\phi = 14 M_{\rm P}$ and $\chi = w(1/2 + 2 * 198)\pi M_{\rm P}$ set $N = 50$ e-folds before the end of inflation. A plot of the spectrum over one oscillation as a function of e-folds from pivot scale $N = 50$.

Explicitly the potential is then of the from

$$
\begin{aligned}
V(\phi) &= \frac{1}{2} m_\phi^2 \phi^2 \,, \\
V(\chi) &= V_0 \left(1 + b \left(\frac{\chi - \chi_0}{\chi_0} \right) + c \left(\frac{\chi - \chi_0}{\chi_0} \right)^3 + d \left(\frac{\chi - \chi_0}{\chi_0} \right)^4 \right) \,, \qquad \chi > \chi_m \\
V(\chi) &= \frac{1}{2} m_\chi^2 \chi^2 \,, \qquad \chi < \chi_m \,.
\end{aligned}
\tag{4.3}
$$

In this case as a concrete example we generate observable results evaluated on the pivot scale with initial conditions $\phi^* = 14 M_{\rm P}$, $\chi_* = \chi_0 = 0.05 M_{\rm P}$, and parameter values $m_\phi = 5 m_\chi$, $V_0 b/\chi_0 = m_\phi^2 \chi_0$ and $\chi_m = 0.049 M_{\rm P}$. The initial value of χ is therefore at the inflection point. We do so for a series of values of $V_0 c/\chi_0^3$ in the range $\{0, 0.01\}$. In contrast with the example above, therefore, we enforce 50 e-folds for a series of different model parameters and plot how the observables evolve with the parameters, rather than as a function of scale.

The results for, n_s, α, $f_{\rm NL}$ and $g_{\rm NL}$ at the point the derivates of N are equal are shown in Fig. 5 together with the analytical estimates where appropriate, r always takes value $r \approx 0.08$. As above, one can clearly see the correlation between a large running and the enhanced $g_{\rm NL}$.

5 Conclusions

The unprecedented accuracy of cosmological surveys opens up new possibilities to probe inflationary physics through correlated patterns of several observables. After the possible hints of primordial gravitational waves in BICEP2 data there has been a significant interest towards running of the spectral index. An eventual detection of large amplitude primordial gravitational waves would favour a large negative running to alleviate tension with the accurate

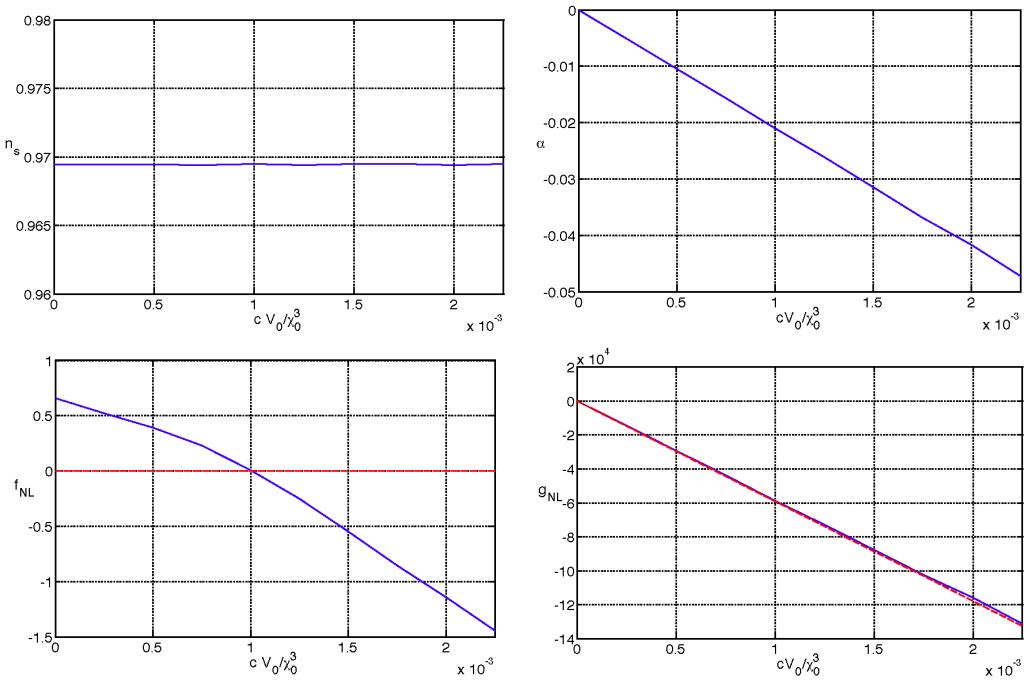

Figure 5. Results for the piecewise isocurvature potential eq. (4.3). Parametric scan of the pivot scale values ($N = 50$) of n_s (top left), r (top right), $f_{\rm NL}$ (bottom left solid), the estimate of $f_{\rm NL}$ (bottom right dashed), $g_{\rm NL}$ (bottom right solid) and the estimate of $g_{\rm NL}$ (bottom right dashed). The results are shown as a function of the parameter combination cV_0/χ_0^3 and measured at the point $N_\phi = N_\chi$.

Planck measurements of the spectral index at high multipoles. While the current BICEP2 data appears compatible with dust [4] the possibility for a large tensor to scalar ratio r and large running α_s is certainly still allowed by observations. The combined analysis BICEP2 and Planck data and the new data from successors of BICEP2 is expected to clarify the situation in near future. It is therefore interesting to investigate the physical ramifications of a large running in more detail.

In this work we have found new possibilities to discriminate between inflaton and curvaton fields including through correlated signatures in scale dependence of the spectral index and non-Gaussian statistics. In both cases a large running of the spectral index can be generated by features in the scalar field potential. Using a simple two parameter description for a local feature either in the inflaton or curvaton potential we have investigated the observational signatures allowing for mixed inflaton and curvaton perturbations. We have shown that a curvaton field generating a large running of the spectral index also necessarily induces a specific non-Gaussian signature in the form of an enhanced trispectrum amplitude $g_{\rm NL}$ peaked around the feature scale. If the curvaton induced running is of the same order as the spectral index $|\alpha_s| = \mathcal{O}(n_s - 1)$ we find the parametric relation $|g_{\rm NL}| = \mathcal{O}(f_{\rm NL}^2/(n_s - 1))$ between the peak values of $g_{\rm NL}$ and the bispectrum amplitude $f_{\rm NL}$. There is no such amplification if the running is generated by the inflaton(s). Thus the correlated signatures of running and non-Gaussianities provide a novel and potentially very useful probe of isocurvature fields present during inflation. This signature is expected no matter what the amplitude of gravitational waves.

Another interesting difference concerns the behaviour of the spectrum away from the feature in cases where a large running is accompanied by an observable value of the tensor to scalar ratio, r. In the inflaton case a single feature generating a large running $\alpha_s = -\mathcal{O}(n_s - 1)$ would rapidly lead to breakdown of slow roll dynamics. A self-consistent setup therefore requires additional structure which levels out the potential within $N \sim 10$ e-folds and brings the spectral index closer to unity. For curvaton induced running due to a single feature, the inflationary dynamics is not affected and the curvaton can stay in the vicinity of the feature resulting a decreasing spectral index over a period up to $N \sim 30$ e-folds. Beyond this regime the potential either needs to be levelled out by additional structure or the curvaton will not stay an isocurvature field. If a large running and r are observed, therefore, and such a levelling out ruled out within $N \sim 10$, the origin would have to be an isocurvature field.

These considerations serve to emphasise the importance of a careful treatment of the second order effects and their correlated behaviour. They could help to uncover potential features and facilitate differentiation between models for the primordial perturbation. As argued here, measuring the running of the spectral index would be very useful in this regard. Correlated with the non-Gaussian statistics, the scaling of the spectrum provides an additional observational tool to discriminate between curvatons and inflatons. To determine the running more accurately, the widening of the observable window of e-folds would be highly desirable. Interestingly, such a possibility might be in the offing by future surveys, which will measure spectral distortions of the CMB and probe the spectrum over a range of up to 17 e-folds.

Acknowledgments

D.J.M. is supported by a Royal Society University Research Fellowship, and was supported by the Science and Technology Facilities Council grant ST/J001546/1 during the majority of this work. He thanks Helsinki for hospitality during the initial stages of this work. SN is supported by the Academy of Finland grant 257532. KE is supported by the Academy of Finland grants 1263714 and 1218322.

References

[1] **Planck Collaboration** Collaboration, P. Ade *et. al.*, *Planck 2013 results. XVI. Cosmological parameters*, arXiv:1303.5076.

[2] **Planck Collaboration** Collaboration, P. Ade *et. al.*, *Planck 2013 results. XXII. Constraints on inflation*, arXiv:1303.5082.

[3] **Planck Collaboration** Collaboration, P. Ade *et. al.*, *Planck 2013 Results. XXIV. Constraints on primordial non-Gaussianity*, arXiv:1303.5084.

[4] **BICEP2 Collaboration** Collaboration, P. Ade *et. al.*, *Detection of B-Mode Polarization at Degree Angular Scales by BICEP2*, *Phys.Rev.Lett.* **112** (2014) 241101, [arXiv:1403.3985].

[5] Z. Hou, C. Reichardt, K. Story, B. Follin, R. Keisler, *et. al.*, *Constraints on Cosmology from the Cosmic Microwave Background Power Spectrum of the 2500-square degree SPT-SZ Survey*, *Astrophys.J.* **782** (2014) 74, [arXiv:1212.6267].

[6] K. Enqvist, T. Meriniemi, and S. Nurmi, *Generation of the Higgs Condensate and Its Decay after Inflation*, *JCAP* **1310** (2013) 057, [arXiv:1306.4511].

[7] J. Espinosa, G. Giudice, and A. Riotto, *Cosmological implications of the Higgs mass measurement*, *JCAP* **0805** (2008) 002, [arXiv:0710.2484].

[8] M. Herranen, T. Markkanen, S. Nurmi, and A. Rajantie, *Spacetime curvature and the Higgs stability during inflation*, *Phys.Rev.Lett.* **113** (2014), no. 21 211102, [arXiv:1407.3141].

[9] K. Enqvist, T. Meriniemi, and S. Nurmi, *Higgs Dynamics during Inflation*, *JCAP* **1407** (2014) 025, [arXiv:1404.3699].

[10] M. Fairbairn and R. Hogan, *Electroweak Vacuum Stability in light of BICEP2*, *Phys.Rev.Lett.* **112** (2014) 201801, [arXiv:1403.6786].

[11] A. Kobakhidze and A. Spencer-Smith, *Electroweak Vacuum (In)Stability in an Inflationary Universe*, *Phys.Lett.* **B722** (2013) 130–134, [arXiv:1301.2846].

[12] A. De Simone and A. Riotto, *Cosmological Perturbations from the Standard Model Higgs*, *JCAP* **1302** (2013) 014, [arXiv:1208.1344].

[13] P. H. De Simone, A. and A. Riotto, *Non-Gaussianities from the Standard Model Higgs*, *JCAP* **1301** (2013) 037, [arXiv:1210.6618].

[14] K. Enqvist and M. S. Sloth, *Adiabatic CMB perturbations in pre - big bang string cosmology*, *Nucl.Phys.* **B626** (2002) 395–409, [hep-ph/0109214].

[15] D. H. Lyth and D. Wands, *Generating the curvature perturbation without an inflaton*, *Phys.Lett.* **B524** (2002) 5–14, [hep-ph/0110002].

[16] T. Moroi and T. Takahashi, *Effects of cosmological moduli fields on cosmic microwave background*, *Phys.Lett.* **B522** (2001) 215–221, [hep-ph/0110096].

[17] A. D. Linde and V. F. Mukhanov, *Nongaussian isocurvature perturbations from inflation*, *Phys.Rev.* **D56** (1997) 535–539, [astro-ph/9610219].

[18] S. Mollerach, *Isocurvature Baryon Perturbations and Inflation*, *Phys.Rev.* **D42** (1990) 313–325.

[19] G. Dvali, A. Gruzinov, and M. Zaldarriaga, *A new mechanism for generating density perturbations from inflation*, *Phys.Rev.* **D69** (2004) 023505, [astro-ph/0303591].

[20] L. Kofman, *Probing string theory with modulated cosmological fluctuations*, astro-ph/0303614.

[21] D. H. Lyth, *Generating the curvature perturbation at the end of inflation*, *JCAP* **0511** (2005) 006, [astro-ph/0510443].

[22] D. H. Lyth, C. Ungarelli, and D. Wands, *The Primordial density perturbation in the curvaton scenario*, *Phys.Rev.* **D67** (2003) 023503, [astro-ph/0208055].

[23] M. Sasaki, J. Valiviita, and D. Wands, *Non-Gaussianity of the primordial perturbation in the curvaton model*, *Phys.Rev.* **D74** (2006) 103003, [astro-ph/0607627].

[24] K. Enqvist and S. Nurmi, *Non-gaussianity in curvaton models with nearly quadratic potential*, *JCAP* **0510** (2005) 013, [astro-ph/0508573].

[25] K. Enqvist, S. Nurmi, O. Taanila, and T. Takahashi, *Non-Gaussian Fingerprints of Self-Interacting Curvaton*, *JCAP* **1004** (2010) 009, [arXiv:0912.4657].

[26] T. Kobayashi, F. Takahashi, T. Takahashi, and M. Yamaguchi, *Spectator field models in light of spectral index after Planck*, *JCAP* **1310** (2013) 042, [arXiv:1303.6255].

[27] K. Enqvist and T. Takahashi, *Mixed Inflaton and Spectator Field Models after Planck*, *JCAP* **1310** (2013) 034, [arXiv:1306.5958].

[28] J. Ellis, M. Fairbairn, and M. Sueiro, *Rescuing Quadratic Inflation*, *JCAP* **1402** (2014) 044, [arXiv:1312.1353].

[29] J. Meyers and E. R. M. Tarrant, *Perturbative Reheating After Multiple-Field Inflation: The Impact on Primordial Observables*, *Phys.Rev.* **D89** (2014) 063535, [arXiv:1311.3972].

[30] C. T. Byrnes, M. Corts, and A. R. Liddle, *Comprehensive analysis of the simplest curvaton model*, *Phys.Rev.* **D90** (2014), no. 2 023523, [arXiv:1403.4591].

[31] E. D. Stewart, *The Spectrum of density perturbations produced during inflation to leading order in a general slow roll approximation*, *Phys.Rev.* **D65** (2002) 103508, [astro-ph/0110322].

[32] F. Takahashi, *The Spectral Index and its Running in Axionic Curvaton*, *JCAP* **1306** (2013) 013, [arXiv:1301.2834].

[33] M. S. Sloth, *Chaotic inflation with curvaton induced running*, arXiv:1403.8051.

[34] **Planck Collaboration** Collaboration, R. Adam *et. al.*, *Planck intermediate results. XXX. The angular power spectrum of polarized dust emission at intermediate and high Galactic latitudes*, arXiv:1409.5738.

[35] **BICEP3 Collaboration** Collaboration, Z. Ahmed *et. al.*, *BICEP3: a 95GHz refracting telescope for degree-scale CMB polarization*, *Proc.SPIE Int.Soc.Opt.Eng.* **9153** (2014) 91531N, [arXiv:1407.5928].

[36] C. Sheehy, P. Ade, R. Aikin, M. Amiri, S. Benton, *et. al.*, *The Keck Array: a pulse tube cooled CMB polarimeter*, arXiv:1104.5516.

[37] J. Lazear, P. A. R. Ade, D. Benford, C. L. Bennett, D. T. Chuss, *et. al.*, *The Primordial Inflation Polarization Explorer (PIPER)*, *Proc.SPIE Int.Soc.Opt.Eng.* **9153** (2014) 91531L, [arXiv:1407.2584].

[38] A. Fraisse, P. Ade, M. Amiri, S. Benton, J. Bock, *et. al.*, *SPIDER: Probing the Early Universe with a Suborbital Polarimeter*, *JCAP* **1304** (2013) 047, [arXiv:1106.3087].

[39] K. N. Abazajian, G. Aslanyan, R. Easther, and L. C. Price, *The Knotted Sky II: Does BICEP2 require a nontrivial primordial power spectrum?*, arXiv:1403.5922.

[40] S. Dodelson and E. Stewart, *Scale dependent spectral index in slow roll inflation*, *Phys.Rev.* **D65** (2002) 101301, [astro-ph/0109354].

[41] T. Kobayashi and F. Takahashi, *Running Spectral Index from Inflation with Modulations*, *JCAP* **1101** (2011) 026, [arXiv:1011.3988].

[42] M. Czerny, T. Kobayashi, and F. Takahashi, *Running Spectral Index from Large-field Inflation with Modulations Revisited*, arXiv:1403.4589.

[43] S. Clesse, B. Garbrecht, and Y. Zhu, *Testing Inflation and Curvaton Scenarios with CMB Distortions*, arXiv:1402.2257.

[44] D. Lyth, *Large Scale Energy Density Perturbations and Inflation*, *Phys.Rev.* **D31** (1985) 1792–1798.

[45] A. A. Starobinsky, *Multicomponent de Sitter (Inflationary) Stages and the Generation of Perturbations*, *JETP Lett.* **42** (1985) 152–155.

[46] D. Wands, K. A. Malik, D. H. Lyth, and A. R. Liddle, *A New approach to the evolution of cosmological perturbations on large scales*, *Phys.Rev.* **D62** (2000) 043527, [astro-ph/0003278].

[47] M. Sasaki and E. D. Stewart, *A General analytic formula for the spectral index of the density perturbations produced during inflation*, *Prog.Theor.Phys.* **95** (1996) 71–78, [astro-ph/9507001].

[48] D. H. Lyth and Y. Rodriguez, *The Inflationary prediction for primordial non-Gaussianity*, *Phys.Rev.Lett.* **95** (2005) 121302, [astro-ph/0504045].

[49] J. Elliston, D. J. Mulryne, D. Seery, and R. Tavakol, *Evolution of fNL to the adiabatic limit*, *JCAP* **1111** (2011) 005, [arXiv:1106.2153].

[50] J. Elliston, D. J. Mulryne, and R. Tavakol, *What Planck does not tell us about inflation*, *Phys.Rev.* **D88** (2013) 063533, [arXiv:1307.7095].

[51] E. Sefusatti, M. Liguori, A. P. Yadav, M. G. Jackson, and E. Pajer, *Constraining Running Non-Gaussianity*, *JCAP* **0912** (2009) 022, [arXiv:0906.0232].

[52] C. T. Byrnes, M. Gerstenlauer, S. Nurmi, G. Tasinato, and D. Wands, *Scale-dependent non-Gaussianity probes inflationary physics*, *JCAP* **1010** (2010) 004, [arXiv:1007.4277].

[53] C. T. Byrnes, S. Nurmi, G. Tasinato, and D. Wands, *Scale dependence of local f_{NL}*, *JCAP* **1002** (2010) 034, [arXiv:0911.2780].

[54] C. T. Byrnes and G. Tasinato, *Non-Gaussianity beyond slow roll in multi-field inflation*, *JCAP* **0908** (2009) 016, [arXiv:0906.0767].

[55] S. Shandera, N. Dalal, and D. Huterer, *A generalized local ansatz and its effect on halo bias*, *JCAP* **1103** (2011) 017, [arXiv:1010.3722].

[56] A. D. Linde and V. Mukhanov, *The curvaton web*, *JCAP* **0604** (2006) 009, [astro-ph/0511736].

[57] K. A. Malik and D. H. Lyth, *A numerical study of non-gaussianity in the curvaton scenario*, *JCAP* **0609** (2006) 008, [astro-ph/0604387].

[58] J. Elliston, S. Orani, and D. J. Mulryne, *General analytic predictions of two-field inflation and perturbative reheating*, *Phys.Rev.* **D89** (2014) 103532, [arXiv:1402.4800].

[59] J. Elliston, L. Alabidi, I. Huston, D. Mulryne, and R. Tavakol, *Large trispectrum in two-field slow-roll inflation*, *JCAP* **1209** (2012) 001, [arXiv:1203.6844].

[60] J. Ellis, N. E. Mavromatos, and D. J. Mulryne, *Exploring Two-Field Inflation in the Wess-Zumino Model*, *JCAP* **1405** (2014) 012, [arXiv:1401.6078].